Cellular models for river networks

Guido Caldarelli
INFM, Sezione di Roma 1, Dipartimento di Fisica, Università di Roma ''La Sapienza,'' Piazzale Aldo Moro 2, 00185 Roma, Italy
(Received 27 June 2000; revised manuscript received 22 September 2000; published 26 January 2001)

A cellular model introduced for the evolution of the fluvial landscape is revisited using extensive numerical and scaling analyses. The basic network shapes and their recurrence especially in the aggregation structure are then addressed. The roles of boundary and initial conditions are carefully analyzed as well as the key effect of quenched disorder embedded in random pinning of the landscape surface. It is found that the above features strongly affect the scaling behavior of key morphological quantities. In particular, we conclude that randomly pinned regions (whose structural disorder bears much physical meaning mimicking uneven landscape-forming rainfall events, geological diversity or heterogeneity in surficial properties like vegetation, soil cover or type) play a key role for the robust emergence of aggregation patterns bearing much resemblance to real river networks.

DOI: 10.1103/PhysRevE.63.021118 PACS number(s): 05.40.−a, 68.70.+w

I. INTRODUCTION

Through experimental studies, it has become evident in the past few years that the geometrical and topological structures of river basins are characterized by the absence of a single well-defined length scale. This is reflected in the appearance of power laws in the distribution of several quantities, chiefly total contributing area at a point [1] and stream lengths [2–5], and by the clear experimental assessment of scaling properties (yielding either self-similarity or self-affinity [6]) for many geometrical descriptors of the river basin [7–9]. The discovery of the general underlying mechanisms yielding scale-free features is the present theoretical challenge.

The network associated with a given natural terrain pertaining to a river basin can be experimentally analyzed by using the so-called digital elevation map technique [2,9–13] that allows to determine the average height of areas (pixels) of the order 10^{-2} Km^2. Thus a fluvial basin is represented in an objective manner often over four logarithm scales of linear size. Lower bounds are imposed by channel initiation processes at O(10–100) m. Crossovers of geological nature provide altered aggregation processes and thus an upper cutoff, usually beyond scales of $O(10^5–10^6)$ m. Thus the observational evidence yields a much more reliable framework over many scales for comparison with dynamical models aimed at the origin of scale-free features.

Much interest has been recently attracted by landscape evolution models. Chief among those are the detailed deterministic models that address the description of the detailed dynamics acting on the landscapes [14]. The reductionist approach, where a precise description of the details of the dynamics is sought, is successful, and much interesting, in the pursuit of the description and the classification of landforms. Nevertheless, as standard in critical phenomena, the mechanism producing scale-free structures is expected to depend only on a few key features common to all the networks rather than on the details of the particular system under study. Hence in this work, centered on the dynamic origin of fractal river networks, we follow a nonreductionist approach based on the simplest possible, parameter-free models capable of allowing the emergence of complexity.

A flow-rate unit is associated with each pixel and the flow contributing to any pixel follows the steepest descent path through drainage directions whose collection defines the planar structure under consideration. The resulting network is therefore the two-dimensional projection of the three-dimensional treelike structure of the steepest descent paths draining a given basin. The planar patterns of network aggregation are obtained by employing the cellular model for the evolution of a fluvial landscape originally introduced by [15] and further studied in [16]. It is aimed at describing in a crucially simple manner the sole fluvial component of landscape evolution. Although such component must be coupled to other—chiefly hillslope—transport processes to yield a comprehensive dynamical description [11,14,17–19], it rules the planar imprinting of the network. Hence the detailed study of the model is deemed significant.

Starting from a three-dimensional landscape, evolution occurs according to a threshold dynamics similar to the one proposed in self-organized critical (SOC) models [20]. The main idea of the erosion dynamics is that whenever the local shear stress exceeds a given threshold, erosion starts an ''avalanche'' and a related rearrangement of the network patterns takes place. The model of self-organizing fluvial structures may be seen as a modification of the sandpile model developed as a paradigm of the dynamics of open, dissipative systems with many degrees of freedom. It may be thought of as belonging to the set of models in which the threshold for activity, say τ_c, rather than being a constant value, depends on nonlocal properties of the self-organizing structure. In the fluvial case, the nonlocal character of the threshold value follows from the fact that the threshold at the arbitrary site equals a shear stress, i.e., $\tau \propto \nabla h \sqrt{a}$, where h is the local landscape elevation and a is total contributing area surrogating total flow collected from a distributed rainfall event. As such, the exceeding of τ_c depends not only on local conditions (i.e., a critical value of ∇h), but also on nonlocal conditions defined by the contributing area a computed through drainage directions, i.e., it depends on the entire state of the system that is self-organizing. Notice that the physical rationale for the nonlocal dependence lies in the fact

 ©2001 The American Physical Society

that the system is open, i.e., injected from outside, allowing flow rates to be proportional to total contributing drainage area. The long-range nature of the threshold dynamics tends to hide from the observer the temporal fluctuations that take place in the evolutionary time scale. In this sense the above model was classified [15] as one of spatial self-organized criticality.

Whether or not river self-organization qualifies as a more general framework of self-organized criticality remains to be seen. If SOC must necessarily refer to the occurrence of a critical state in the sense of critical phenomena, where a small local perturbation can cause a significant change in the configuration of the whole system and thus the system shows both spatial and temporal scaling, then the time dynamics should be specifically considered. One way to do this is through the oscillation of the threshold in time, i.e., $\tau_c(t)$, simulating climatic fluctuations (see [21]), through which indeed temporal evolution appears, or through perturbations of random location and strength in the evolution of the landscape. This is also true, as we will discuss later, if the landscape-forming rainfall events are described as nonuniform in space, leading to patches of activity randomly scattered spatially (in such a case the outflow response of the system becomes a $1/f$ signal). However, regardless of any additional features, we believe that the central scope of SOC is the dynamic explanation of the growth of fractal structures of the type appearing in nature, i.e., the physics of fractals. As such we feel that our classification of the model as a particular case of SOC is a suitable one regardless of the description of the embedded temporal activity because the system always reaches a fractal state. Moreover, questioning on this basis [23] the self-organized critical nature of the model by Ref. [15] is irrelevant because it has been shown on thermodynamics grounds that scaling properties of energy and entropy yield limit states which, depending on the constraints, are temporally frozen or active [5]. Furthermore, Ref. [9] shows that optimal states like the ones dynamically accessed by the above model may exist in temporally active states precisely at the edge of a chaotic behavior.

A question, indeed more interesting than the semantics of SOC, is whether the constraints in the model may be relaxed to produce a ''hot'' fluvial landscape more closely resembling an ordinary sandpile. This question is addressed in [5] and in more detatil in [9].

Our main goal is twofold. On one hand we will extend previous investigations both in accuracy and in statistics by performing simulations at much larger scales. On the other hand, we will consider important issues such as the effect of the boundaries and of the initial conditions bearing much significance on geological influences. In particular we will show that both the aforementioned effects play an important role in the results previously obtained. We also study the effects of disorder, say through the presence of small, uncorrelated inhomogeneities in the initial conditions, in particular with regard to the robustness to single/multiple outlet arrangements.

The paper is organized as follows. In Sec. II, the model is recalled. Section III presents the results with emphasis on scaling analyses, while the following section focuses on the important effects of quenched pinning on the system. Then a set of conclusions closes the paper.

II. THE MODEL

We consider a lattice model of a real landscape. Let h_x be the height of the landscape associated with every site x of a square lattice of size $L\times L$. The lattice is tilted at an angle θ with respect to a given axis to mimic the effects of gravity. Two possibilities will be analyzed

(1) All the sites on the lowest side (kept at height $h=0$) are possible outlets (i.e., the multiple outlet arrangement) of an ensemble of rivers that are competing to drain the whole $L\times L$ basin.

(2) Only one site is kept at $h=0$ and it is the outlet of a single river in the $L\times L$ basin.

In addition, for both the above cases, two types of initial conditions will be considered: (a) a regular initial landscape, e.g., flat, and (b) an irregular surface obtained by superposing a suitable noise on a smooth sloping surface.

Each site collects a unit amount of water from a distributed injection (here a constant rainfall rate as in the original approach) in addition to the flow that drains into it from the upstream sites. A unit of water mass is assigned to each pixel of drainage area so that the total area drained into a site is also a measure of the total water mass collected at that site. From each site water flows to one of the eight sites, four nearest neighbors and four next nearest neighbors, having the lowest height (i.e., the steepest descent path). We shall indicate all these eight neighboring sites as nearest-neighbors (nn). This construction allows the assignment of drainage directions to an arbitrary landscape. The drained area a_x is associated with each site x according to the equation

$$a_x=\sum_{y(x)} a_y+1, \tag{1}$$

where the sum runs over the subset $y(x)\in \mathrm{nn}(x)$ of neighbor sites whose area is actually drained by x. The second term in Eq. (1) represents the uniform injection.

Also, the (up)stream length l_x from site x to the source is computed according to the following procedure. At a given site x the areas of all $\mathrm{nn}(x)$ of that site are checked, following the ordinary meaning of downstream and upstream sites, i.e., downstream is the site one finds following the river to the outlet, upstream is the site following which one reaches the source from which the largest incoming river enters the site. Following Ref. [8], the nn with largest value leads to the outlet and is defined to be a downstream site. The nn with the second largest value indicates the longest path toward the source and is defined to be the upstream site. The sum of all the upstream sites from site x to the source is l_x. The downstream length could be defined through an analogou procedure. Experimental measures are available for both a_x and l_x [9].

The time evolution of the model follows the following steps:

(1) The shear stress τ_x acting at every site is computed according to [15]

$$\tau_x = \Delta h_x \sqrt{a_x} \tag{2}$$

where Δh_x is the local gradient along the drainage direction.

(2) If the shear stress at a site exceeds a threshold value τ_c then the corresponding height h_x is reduced (i.e., by erosion) in order to decrease the local gradient. The shear stress is set just at the threshold value. This produces a rearrangement of the network followed by a reupdating of the whole pattern as in step 1.

(3) When all sites have shear stress below threshold the system is in a dynamically steady state. Since this situation is not necessarily the most stable, a perturbation is applied to the network with the aim of increasing the stability of a new steady state. A site is thus chosen at random and its height is increased in such a way that no lakes, i.e., sites whose height is lower than that of their eight neighbors, are formed. Steps 1 and 2 then follow as before.

After a suitable number of the perturbations (step 3), the system reaches a steady state that is insensitive to further perturbations and where all statistics of the networks are stable. This resulting state is scale-free, i.e., it is characterized by power-law distributions of the physical quantities of interest.

III. RESULTS

A. Landscape evolutions

Our numerical calculations were carried out on a bidimensional square lattice (where each site has eight nearest-neighbors) for sizes up to $L=200$ with reflecting boundary conditions in the direction transversal to the flow and open boundary condition in the parallel one. We considered the following initial conditions

Model A. A comblike structure with a single outlet. This was the situation originally studied in [15] and our results are in agreement with theirs.

Model B. An inclined plane with all sites at the bottom of the plane allowed to be possible outlets. This choice was selected with the aim of investigating the differences arising when arranging the boundary conditions with multiple outlets versus single outlet. The former allows for competition for drainage area among rivers.

Models C and D. The two previously considered situations with the addition of a random, uncorrelated noise (whose strengtht, i.e., variance, is less than 10% of the average height). That is, on top of the height computed according to the rules of model A and B, respectively (a comblike lattice and an inclined plane), we added a random Dh that is extracted in the interval $[-\langle h\rangle/10,\langle h\rangle/10]$ where $\langle h\rangle$ represents the mean altitude of the landscape.

An average over a few (up to five) configurations was taken. This choice, especially when coupled to large sizes of the system, proves sufficient for statistical descriptions sought in view of the self-averaging nature of the random perturbation.

In Fig. 1 typical landscapes sculpted by the above dynamical process and the corresponding networks drawn through the steepest descent construction are shown for models A and B. The same picture for models C and D is shown in Fig. 2.

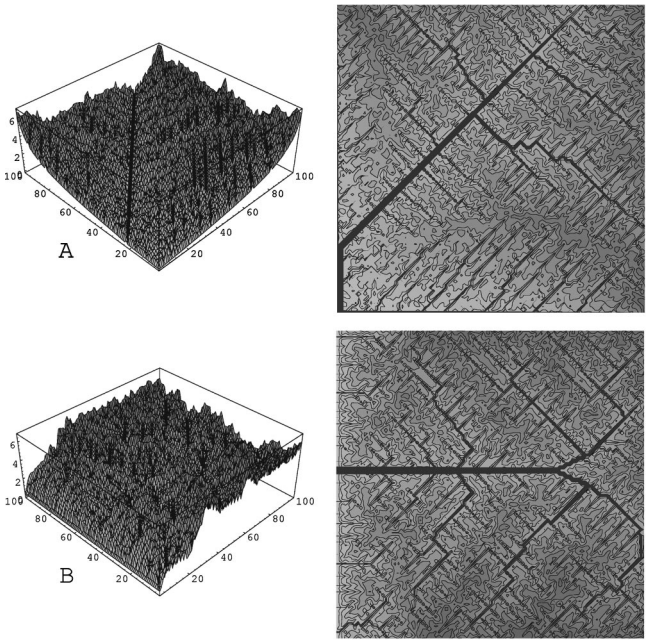

FIG. 1. The final landscape (on the left) and the final network structure (on the right) for model A and model B. Models A and B start from a deterministic initial condition. Model A has single outlet, model B has multiple outlets.

Two features can be grasped from these pictures. First, in the results of both models A and B, there is a strong memory of the initial configuration despite the fact that the dynamics

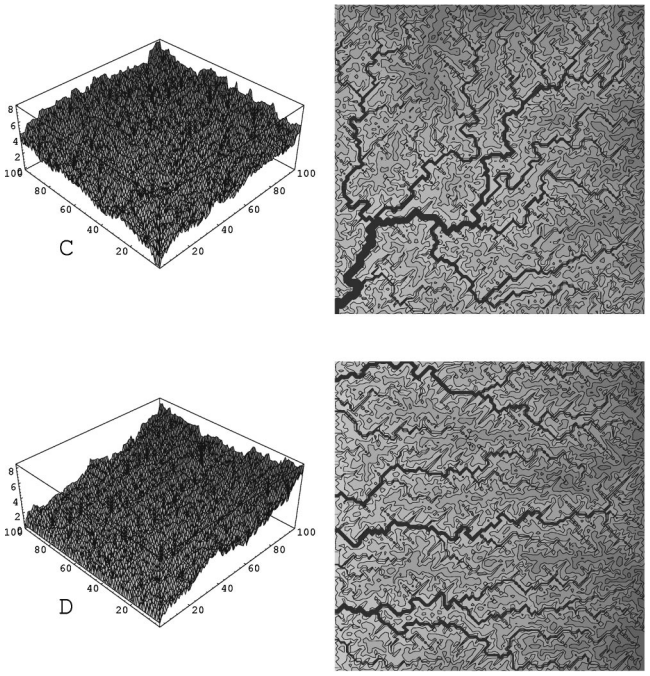

FIG. 2. The final landscape (on the left) and the final network structure (on the right) for model C and model D. Models C and D start from a random initial condition. Model C has single outlet, model D has multiple outlets.

TABLE I. Scaling relations: all the exponents can be determined in terms of d_l in the fractal case and H in the self-affine case.

Exponent	Self-similar	Self-affine
τ	$2-d_l$	$(1+2H)/(1+H)$
γ	$2/d_l$	$1+H$
h	$d_l/2$	$1/(1+H)$

of the erosion process was somewhat expected to be sufficiently strong to soon lose the imprinting of its initial condition. Second, the single outlet restriction imposed in model A appears to be a severe constraint because it increasingly affects the wandering of the main river toward the lowest part of the basin. Our results suggest that this is indeed the case for flat initial conditions (A and B), while for noisy initial-conditions boundary effects are of lesser importance.

B. Area and length exponents

Let us define $P(a,L)$ and $\Pi(l,L)$ as the exceeding (cumulative) probability distributions of the drainage area a and stream length l, respectively, arising in a domain of linear size L. The following scaling forms are expected to hold [8]:

$$P(a,L)=a^{1-\tau}F\left(\frac{a}{L^{1+H}}\right), \tag{3}$$

$$\Pi(l,L)=l^{1-\gamma}G\left(\frac{l}{L^{d_l}}\right). \tag{4}$$

Here H is the Hurst exponent [6] and d_l is the stream-length (or chemical distance) fractal exponent.

As it was already noted [8], for self-affine river networks ($H<1, d_l=1$), the scaling relations relate all exponents in terms of H. For self-similar river networks ($H=1, d_l>1$), the same happens in terms of d_l.

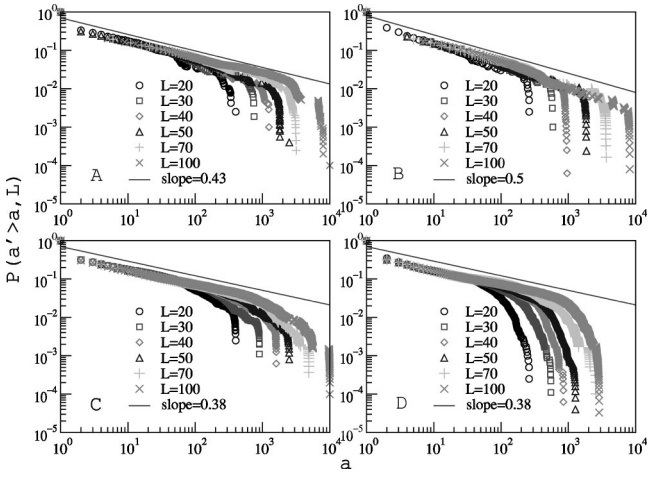

FIG. 3. Log-log plot of the area cumulated distribution $P(a,L)$ versus a for models A, B, C, and D. The full line has a slope corresponding to $\tau=1.43$, $\tau=1.50$, $\tau=1.38$, and $\tau=1.38$, respectively.

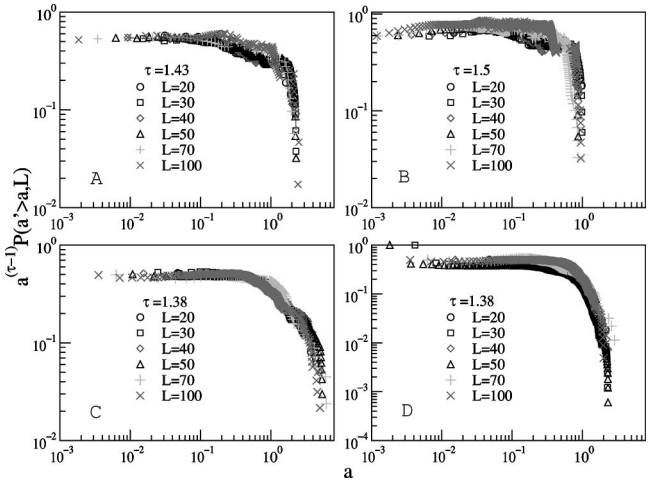

FIG. 4. Scaling function $a^{1-\tau}P(a,L)$ versus a/L^{1+H} for model C. The used values to obtain the collapse were $\tau=1.43$, $\tau=1.5\tau=1.38$, and $\tau=1.38$ for models A, B, C, D, respectively. $H=0.6$ in all the cases.

Another important indicator of basin morphology is the relation between the mean total contributing area a and the length of the main stream $l_{\max}\propto L^{d_l}$ [8,24], which is commonly known as Hack's law [22]:

$$a\propto l_{max}^{1/h}\propto L^{d_l/h}. \tag{5}$$

The related exponent has been studied in all simulations. A summary of the scaling relations between the various exponents involved is reported in Table I.

Experimental values of τ and γ are available from earlier analyses of DTMs from basins of different size, geology, exposed lithology, climate, and vegetation [1,24]. It was observed that, while a majority of basins tend to seemingly universal values $\tau=1.43\pm0.02$ and $\gamma=1.8\pm0.1$, exceptions are observed where altered values are observed although always in a concerted manner. Since it was suggested [8] that scaling laws for river networks are related, e.g., $\gamma=1+(\tau-1)/h$, it was concluded there that no universal exponents are expected in nature. Rather, the roles of geology and tectonics concert a coordinated scaling structure that strives for fractality yet adapted to its geological environment. The results of the model described here, revisited in the above light, conform to this view.

The results for the four models A, B, C, and D for the area distributions are shown in Fig. 3. It is apparent that due to the pathological initial conditions the scaling behavior for models A and B is somewhat more noisy than for models C and D. Figure 4 contains the collapse plot for all the cases. Figure 5 shows the stream-length distribution for the four models. For this picture the same remarks of Fig. 3 apply. In Fig. 6 we show the collapse plot corresponding to the stream-length distributions.

A summary of the scaling exponents obtained is included in Table II, where we observe a consistent picture of related scaling exponents as theoretically expected: see Table I.

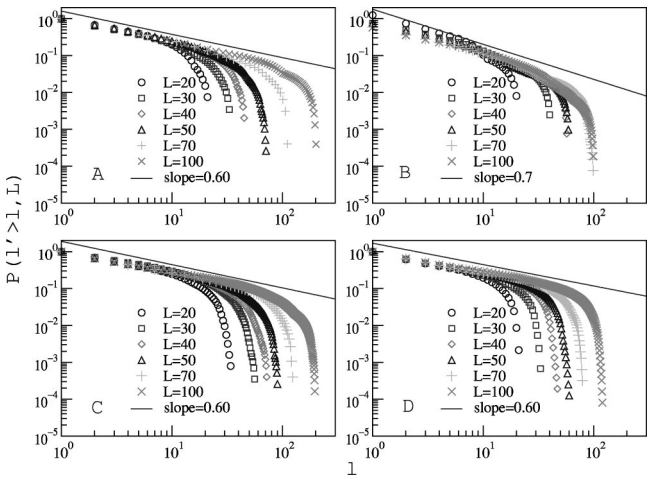

FIG. 5. Log-log plot of the length cumulated distribution $P(l,L)$ versus l for models A, B, C, and D. The full line has a slope corresponding to $\gamma=1.6$, $\gamma=1.7$, $\gamma=1.6$, and $\gamma=1.6$, respectively.

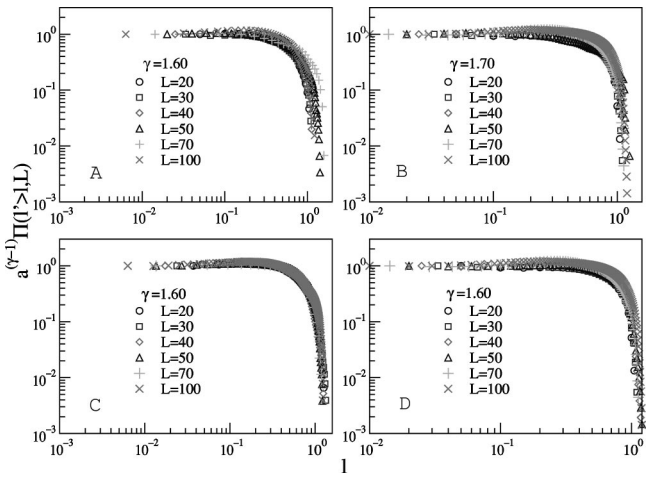

FIG. 6. Scaling function $l^{1-\gamma}\Pi(l,L)$ versus l/L^{d_l} for models A, B, C, and D. The values used to obtain the collapse were to $\gamma=1.6$, $\gamma=1.7$, $\gamma=1.6$, and $\gamma=1.6$, respectively.

C. Energy dissipation and optimal channel networks

During the evolution of the landscape we also monitored the change in total energy dissipation of the system, defined as $E=\Sigma_x a_x^{0.5}$ (where x spans all sites of the lattice) [25–27]. The reason of this name come from the computation at any site of the gravitational energy lost by the falling of the water. In any point x, one can expect a gravitational energy loss of the order of $a_x \Delta h_x$ where Δh_x represents the local gradient along the drainage direction. By using the observed scaling $\Delta h_x \propto a_x^{0.5}$ one obtains the above formula. The interest in this quantity comes from the fact that an extensive class of models known as optimal channel network (OCN) models, assumed this quantity is minimized by natural landscape evolution. By using this principle, OCN described evolution from random spanning graphs to network more similar to the real ones. It is interesting to note that in this model where no hypothesis is made on E, we still observe an almost monotonical decrease of E associated with the dynamical evolutions, and a stabilization on different plateaus of values of E. The actual figures for a sample 30 are as follows: E starts from an initial value of 7600 and decreases towards a plateau of 6800–6700 where this monotonic decrease becomes slower (1% decrease in 50 000 steps). This behavior, also observed in other models [28], bears important consequences in the light of the suggested connection of fractality and optimality [5,25–27]

IV. GEOLOGICAL CONSTRAINTS AND QUENCHED RANDOM PINNING

This section presents a detailed study on the effects on landcape evolution of quenched randomness, simulated by a random choice of sites unable to evolve regardless of the threshold value developed therein. It is found that this form of disorder tends to favor aggregation patterns characterized by values of $\tau=1.43\pm0.02$ for both models, say, A and B (i.e., with single outlets or open boundary conditions). These results suggest that the origin of the recurrent values observed in nature could be related to the ubiquity of heterogeneity in surface properties characterizing locally the critical shear threshold.

Within the river basin, morphological and geological constraints play a definite role in the dynamical evolution of landforms. The effects of quenched constraints, simulating any heterogeneity in the distribution of surficial properties affecting erosion properties, are to favor some sites for the flowpaths, thus excluding other sites from the capture of the developing network that ultimately shapes the evolution process. In order to mimic such effects we analyzed the effect of a random pinning of a small region of the total surface (typically 5–9 %) where the evolution is frozen, that is, the height is pinned to its initial value. We find that this constraint tends to favor aggregation even in the presence of random initial conditions.

As regards the effect of the pinning, Fig. 7 (on the left) shows a sample whose dimension is 100 with multiple outlet and random initial noise (model D). Figure 7 (on the right) shows the same configuration (evolved from the same initial conditions) but with a 5% dilution pinning. It is evident that some of the smaller streams on the left have increased their size thus leading to a bigger aggregation.

In this case we found $\tau=1.43\pm0.02$. Moreover, all the other exponents verify the correct scalings predicted in Table I. Purely for comparison purposes with the previous results, we also report the plot of the area distribution in Fig. 8 on the left. We also found that model D reproduces the same

TABLE II. Data computed for the various computer simulations. Since the scaling relationship $h=(\tau-1)/(\gamma-1)$ one can also compute the theoretical value h_{ex} with the measured one h_{ex}. The agreement of the two is rather good.

	Model A	Model B	Model C	Model D
τ	1.43 ± 0.03	1.50 ± 0.03	1.38 ± 0.02	1.38 ± 0.02
γ	1.60 ± 0.05	1.70 ± 0.05	1.60 ± 0.02	1.60 ± 0.02
h_{th}	0.72 ± 0.05	0.71 ± 0.05	0.63 ± 0.05	0.63 ± 0.05
h_{ex}	0.72 ± 0.05	0.69 ± 0.02	0.65 ± 0.02	0.65 ± 0.02

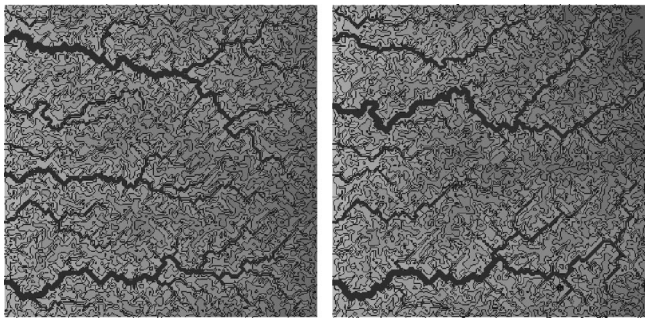

FIG. 7. Comparison between the evolution of two identical initial configurations of model C with size $L=100$ without (left) and with pinning (right). The pinning dilution was 5%.

results, i.e., $\tau=1.43\pm0.04$ and $\gamma=1.60\pm0.04$. We are confident that this result at least for model C is quite robust with respect to changes of the pinning dilution. In the case of a 9% dilution for a smaller number of simulation we found quite similar results $\tau=1.44\pm0.05$ and a cumulative plot of $P(a'>a,L)$ is shown on the right part of Fig. 8 [29].

This result suggests that the origin of recurrent values observed in nature could indeed be related to the ubiquity of geological and morphological constraints in the surface properties locally characterizing the critical shear stress.

V. CONCLUSIONS

In this paper we revisited the model originally introduced in [15] that we extended both in accuracy and goals. Specifically, we analyzed the stability of the universality class of the original model with respect to the initial conditions and to the change from single to multiple outlets. We found that if one starts with structured initial conditions, critical exponents are sensible to a change from single to multiple outlets. On the other hand, upon starting from disordered initial conditions, we found critical exponents belonging to a new class that appears to be robust to the change from single to multiple outlet. Thus this simple model, under controlled conditions, yields somewhat different yet internally consistent scale-free fluvial landforms depending on the dominant conditions affecting evolution.

The above results conform to the experimental observation [8], suggesting that the relevant scaling exponents for river networks are not universal. Rather, the fractal nature of river networks adjusts to the constraints imposed by the geological environment in a coordinated manner. It is interesting to observe that the final state of all simulation yields indeed fractal structures, as observed in nature, though characterized by different aggregation properties. The exponents characterizing these different aggregates, nevertheless follow

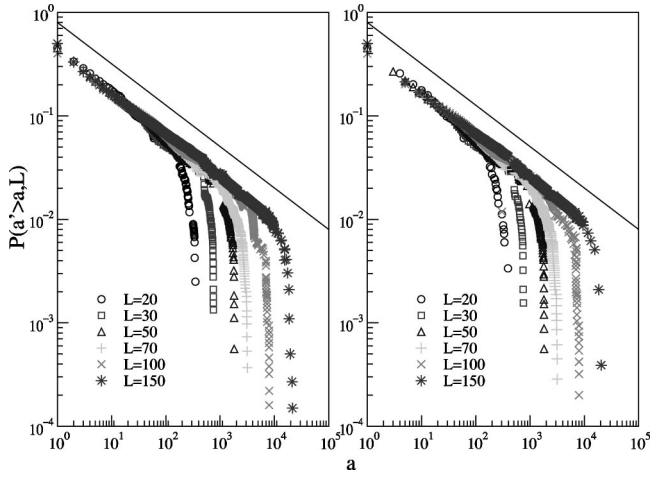

FIG. 8. Log-log plot of the area distribution $P(a,L)$ vs a for model C with a 5% dilution (left) and with a 9% dilution (right). The slopes of the lines correspond, respectively, to $\tau=1.43$ and $\tau=1.44$.

in a rather good agreement with the scaling relations shown in Table I.

We suggest that the lack of robustness in the value of the scaling exponents with respect to boundary and initial conditions is related to the nonlocal character of the shear-based threshold, differently from what is observed in classical sandpile models of self-organized criticality [20]. The intrinsic interest of the different aggregation properties of the steady states of the dynamics is related to their optimality with respect of total energy dissipation [15]. In fact, depending on external conditions, the same dynamical process may indeed get trapped in steady-state configurations yielding local minima of the total energy dissipation functional, in what we may define as a feasible optimality process [5].

Finally, we have found that quenched disorder, modeled by random pinning, has a profound effect on the robustness of the resulting planar patterns by favoring aggregation and by locking the planar landforms into modes quite similar to the ones observed in nature.

The remarkable success obtained by such a simple model in enlightening some crucial features of the real basins is promising for a future success in a general characterization of the dynamics of fractal growth.

ACKNOWLEDGMENTS

Enlightening discussions with J. Banavar, F. Colaiori, A. Flammini, A. Maritan, and A. Rinaldo are acknowledged. Suggestions by A. Giacometti have been particularly helpful. The author acknowledges support from EU Contract No. FMRXCT980183.

[1] I. Rodriguez-Iturbe, E. Ijjasz-Vasquez, R.L. Bras, and D.G. Tarboton, Water Resour. Res. **28**, 988 (1992).

[2] D.G. Tarboton, R.L. Bras, and I. Rodriguez-Iturbe, Water Resour. Res. **24**, 1317 (1988).

[3] P. La Barbera and R. Rosso, Water Resour. Res. **25**, 735 (1989).

[4] M. Marani, A. Rinaldo, R. Rigon, and I. Rodriguez-Iturbe, Geophys. Res. Lett. **21**, 2123 (1994).

[5] A. Rinaldo, A. Maritan, A. Flammini, F. Colaiori, R. Rigon, I. Rodriguez-Iturbe, and J.R. Banavar, Phys. Rev. Lett. **76**, 3364 (1996).
[6] J. Feder, *Fractals* (Plenum, New York, 1988).
[7] B. B. Mandelbrot, *The Fractal Geometry of Nature* (Freeman, New York, 1983).
[8] A. Maritan, A. Rinaldo, R. Rigon, A. Giacometti, and I. Rodriguez-Iturbe, Phys. Rev. E **53**, 1510 (1996).
[9] I. Rodriguez-Iturbe and A. Rinaldo, *Fractal River Basins: Chance and Self-Organization* (Cambridge University Press, Cambridge, 1996).
[10] L. Band, Water Resour. Res. **22**, 15 (1986).
[11] W.E. Dietrich, C.J. Wilson, D.R. Montgomery, and J. McKean, J. Geol. **20**, 675 (1992).
[12] D.R. Montgomery and W.E. Dietrich, Nature (London) **336**, 232 (1988).
[13] D.R. Montgomery and W.E. Dietrich, Science **255**, 826 (1992).
[14] A.D. Howard, Water Resour. Res. **30**, 2261 (1994).
[15] A. Rinaldo, I. Rodriguez-Iturbe, R. Rigon, E. Ijjasz-Vasquez, and R.L. Bras, Phys. Rev. Lett. **70**, 822 (1993).
[16] G. Caldarelli, A. Giacometti, A. Maritan, I. Rodriguez-Iturbe, and A. Rinaldo, Phys. Rev. E **55**, R4865 (1997).
[17] G.R. Willgoose, R.L. Bras, and I. Rodriguez-Iturbe, Water Resour. Res. **27**, 1671 (1991).
[18] A. D. Howard, W. E. Dietrich, and M. J. Selby, J. Geophys. Res. **99**, 13 971 (1994).
[19] R. Rigon, A. Rinaldo, and I. Rodriguez-Iturbe, J. Geophys. Res. **99**, 11 971 (1994).
[20] P. Bak, C. Tang, and K. Wiesenfeld, Phys. Rev. Lett. **59**, 381 (1987).
[21] A. Rinaldo, W.E. Dietrich, G.K. Vogel, R. Rigon, and I. Rodriguez-Iturbe, Nature (London) **374**, 632 (1995).
[22] J.T. Hack, U. S. Geol. Surv. Bull. **294-B**, 1 (1957).
[23] V. Sapozhnikov and E. Foufoula-Georgiou, Water Resour. Res. **32**, 1109 (1996).
[24] R. Rigon, I. Rodriguez-Iturbe, A. Giacometti, A. Maritan, D. Tarboton, and A. Rinaldo, Water Resour. Res. **32**, 3367 (1996).
[25] I. Rodriguez-Iturbe, A. Rinaldo, R. Rigon, R.L. Bras, A. Marani, and E.J. Ijjasz-Vasquez, Water Resour. Res. **28**, 1095 (1992).
[26] I. Rodriguez-Iturbe, A. Rinaldo, R. Rigon, R.L. Bras, and E. Ijjasz-Vasquez, Geophys. Res. Lett. **19**, 889 (1992).
[27] A. Rinaldo, I. Rodriguez-Iturbe, I.R. Rigon, R.L. Bras, E. Ijjasz-Vasquez, and A. Marani, Water Resour. Res. **28**, 2183 (1992).
[28] K. Sinclair and R.C. Ball, Phys. Rev. Lett. **76**, 3360 (1996).
[29] Some color pictures relative to the evolution of models A, B, C, D are available at http://pil.phys.uniroma1.it/gcalda/river.html